SCISPACE
formerly Typeset

Open access • Journal Article • DOI:10.1093/MNRAS/STY1302

The luminosities of cool supergiants in the Magellanic Clouds, and the Humphreys-Davidson limit revisited — Source link

Ben Davies, Paul A. Crowther, Emma R. Beasor

Institutions: Liverpool John Moores University, University of Sheffield

Published on: 18 May 2018 - Monthly Notices of the Royal Astronomical Society (Oxford University Press (OUP))

Topics: Luminosity, Supergiant, Metallicity, Stars and Stellar classification

Related papers:

- Rotating massive main-sequence stars - I. Grids of evolutionary models and isochrones
- Mass-loss predictions for O and B stars as a function of metallicity
- Modules for Experiments in Stellar Astrophysics (MESA)
- Modules for experiments in stellar astrophysics (mesa): binaries, pulsations, and explosions
- Studies of luminous stars in nearby galaxies. III. Comments on the evolution of the most massive stars in the Milky Way and the large magellanic cloud

Share this paper:

View more about this paper here: https://typeset.io/papers/the-luminosities-of-cool-supergiants-in-the-magellanic-4qu5p98ogp

LIVERPOOL JOHN MOORES UNIVERSITY

LJMU Research Online

Davies, B, Crowther, PA and Beasor, ER

The luminosities of cool supergiants in the Magellanic Clouds, and the Humphreys-Davidson limit revisited

http://researchonline.ljmu.ac.uk/id/eprint/9363/

Article

Citation (please note it is advisable to refer to the publisher's version if you intend to cite from this work)

Davies, B, Crowther, PA and Beasor, ER (2018) The luminosities of cool supergiants in the Magellanic Clouds, and the Humphreys-Davidson limit revisited. Monthly Notices of the Royal Astronomical Society, 478 (3). pp. 3138-3148. ISSN 0035-8711

LJMU has developed **LJMU Research Online** for users to access the research output of the University more effectively. Copyright © and Moral Rights for the papers on this site are retained by the individual authors and/or other copyright owners. Users may download and/or print one copy of any article(s) in LJMU Research Online to facilitate their private study or for non-commercial research. You may not engage in further distribution of the material or use it for any profit-making activities or any commercial gain.

The version presented here may differ from the published version or from the version of the record. Please see the repository URL above for details on accessing the published version and note that access may require a subscription.

For more information please contact researchonline@ljmu.ac.uk

http://researchonline.ljmu.ac.uk/

Monthly Notices of the ROYAL ASTRONOMICAL SOCIETY

MNRAS **478,** 3138–3148 (2018) doi:10.1093/mnras/sty1302
Advance Access publication 2018 May 18

The luminosities of cool supergiants in the Magellanic Clouds, and the Humphreys–Davidson limit revisited

Ben Davies,[1★] Paul A. Crowther[2] and Emma R. Beasor[1]

[1]*Astrophysics Research Institute, Liverpool John Moores University, Liverpool Science Park ic2, 146 Brownlow Hill, Liverpool L3 5RF, UK*
[2]*Department of Physics and Astronomy, University of Sheffield, Hounsfield Rd, Sheffield S3 7RH, UK*

Accepted 2018 April 17. Received 2018 January 30; in original form 2018 April 17

ABSTRACT

The empirical upper luminosity boundary $L_{\rm max}$ of cool supergiants (SGs), often referred to as the Humphreys-Davidson limit, is thought to encode information on the general mass-loss behaviour of massive stars. Further, it delineates the boundary at which single stars will end their lives stripped of their hydrogen-rich envelope, which in turn is a key factor in the relative rates of Type-II to Type-Ibc supernovae from single star channels. In this paper we have revisited the issue of $L_{\rm max}$ by studying the luminosity distributions of cool SGs in the Large and Small Magellanic Clouds (LMC/SMC). We assemble samples of cool SGs in each galaxy which are highly complete above $\log L/{\rm L}_{\odot}= 5.0$, and determine their spectral energy distributions from the optical to the mid-infrared using modern multiwavelength survey data. We show that in both cases $L_{\rm max}$ appears to be lower than previously quoted, and is in the region of $\log L/{\rm L}_{\odot} = 5.5$. There is no evidence for $L_{\rm max}$ being higher in the SMC than in the LMC, as would be expected if metallicity-dependent winds were the dominant factor in the stripping of stellar envelopes. We also show that $L_{\rm max}$ aligns with the lowest luminosity of single nitrogen-rich Wolf-Rayet stars, indicating of a change in evolutionary sequence for stars above a critical mass. From population synthesis analysis we show that the Geneva evolutionary models greatly overpredict the numbers of cool SGs in the SMC. We also argue that the trend of earlier average spectral types of cool SGs in lower metallicity environments represents a genuine shift to hotter temperatures. Finally, we use our new bolometric luminosity measurements to provide updated bolometric corrections for cool SGs.

Key words: stars: massive – stars: evolution – supergiants.

1 INTRODUCTION

Models of stellar evolution predict that stars with initial masses $M_{\rm init} \geq 8\,{\rm M}_{\odot}$ should swell up to become cool supergiants (SGs) when they leave the main sequence (MS). However, it has long since been established that there is an upper luminosity limit $L_{\rm max}$ above which no cool SGs are observed (Stothers 1969; Sandage & Tammann 1974), now commonly referred to as the Humphreys–Davidson (H–D) limit (Humphreys & Davidson 1979). The existence of this limit implies that the highest mass stars do not evolve to the cool side of the Hertzsprung–Russell (H–R) diagram and instead remain more compact, ending their lives as either blue hypergiants or Wolf-Rayet (WR) stars.

The common interpretation of this luminosity limit is that it is caused by mass-loss, either via a smooth wind, or by episodic Luminous Blue Variable (LBV) type eruptions: the more massive the star, the stronger the mass-loss, resulting in a larger fraction of the star's initial mass being lost prior to core-collapse supernova. Above some initial mass threshold, the entire H-rich envelope can be lost before the star can evolve to the cool side of the H–R diagram, causing it to evolve directly to the WR phase. Just below this mass limit, stars are expected to have a brief cool SG phase before becoming a WR (e.g. Stothers & Chin 1979; Chiosi & Maeder 1986). Therefore, $L_{\rm max}$ is sensitive to the mass-loss rates of stars integrated over their lifetimes.

The most luminous Red Supergiants (RSGs) identified by Humphreys & Davidson (1979) in the Milky Way and Large Magellanic Cloud (LMC) were inferred to have $\log L/{\rm L}_{\odot} = 5.74$ and 5.66, respectively, interpreted as reflecting a genuine limit at $\log L/{\rm L}_{\odot} = 5.8 \pm 0.1$. These measurements of $L_{\rm max}$ relied upon assumed optical bolometric corrections for RSGs, uncertain distances to the Galactic cool SGs, an outdated distance modulus to the LMC, and a selective sample of optically bright stars. Hence, dust-enshrouded cool hypergiants (e.g. van Loon et al. 2005a) would have been missed from their optical study, while those with moderate circumstellar extinction may have had their luminosities under-

★ E-mail: B.Davies@ljmu.ac.uk

© 2018 The Author(s)
Published by Oxford University Press on behalf of the Royal Astronomical Society

Downloaded from https://academic.oup.com/mnras/article-abstract/478/3/3138/4999916 by Liverpool John Moores University user on 24 September 2018

estimated. More recently, determination of bolometric luminosities L_{bol} for the large samples of cool SGs in the MCs has been attempted from atmospheric model fitting (e.g. Levesque et al. 2006, hereafter L06), from which visible and near-infrared (IR) bolometric corrections are obtained (Neugent et al. 2012). However, determining L_{bol} in this way is problematic, due to the presence of circumstellar dust and/or the inherent deficiencies in 1D atmospheric models when used to model highly anisotropic stars (Levesque et al. 2009; Davies et al. 2013).

By focusing exclusively on the Magellanic Clouds (MCs) it is possible to negate the impact of uncertain distances and high foreground extinction.[1] Further, by adding in near- and mid-IR photometry, we can compensate for circumstellar extinction under the assumption that the flux lost at short wavelengths is re-radiated in the mid-IR. We can then obtain bolometric luminosities by directly integrating under the spectral energy distributions. This is possible thanks to extensive photometric surveys of luminous stars in the MCs that have been conducted within recent decades, both visually (Massey 2002; Zaritsky et al. 2002, 2004) and in the near- and mid-IR (Meixner et al. 2006; Wright et al. 2010; Gordon et al. 2011). These surveys have been mined in attempts to obtain statistically complete samples of cool SGs, with hundreds of candidates subsequently being confirmed with spectroscopic follow ups (e.g. Massey & Olsen 2003; Neugent et al. 2012; González-Fernández et al. 2015).

In this paper we take a fresh look at the luminosity distribution of cool SGs in the MCs, with a particular focus on L_{max}. In Section 2 we describe the input catalogues we employ to compile our list of targets, and the multiwavelength photometry we use to determine model-independent luminosities for each target. In Section 3 we then construct model-independent luminosity distributions of cool SGs for both the LMC and SMC. We revisit the issue of L_{max}, compare the luminosity distribution of cool SGs to that of WRs, and to the predictions of evolutionary models. We conclude in Section 4. In the Appendix we also provide a reappraisal of the bolometric corrections of cool SGs.

2 OBSERVATIONAL SAMPLE

2.1 Input catalogues

To compile a list of cool SGs in each of the MCs we have pooled data from several input catalogues, each of which uses a different technique to identify candidate objects. We do this so as to be as complete as possible; dust-enshrouded stars which may be too faint at visible wavelengths to be found in optical surveys may instead show up in mid-IR catalogues. The earliest spectral type we consider is G0, since we wish to separate cool stars from LBV-like objects which may temporarily evolve from the blue to F-types (e.g. R71; Mehner et al. 2013, 2017). Below, we describe the catalogues we have targeted, acknowledging that there is a large degree of overlap between these catalogues.

(i) For optically selected targets, we used Elias, Frogel & Humphreys (1985), Levesque et al. (2006, 2007), and Neugent et al. (2010, 2012), who built upon earlier work of Humphreys (1979a, 1979b) and Massey & Olsen (2003). In each study candidates were selected on the basis of optical colours and brightnesses, and were confirmed with follow-up spectroscopy.

(ii) For near-IR bright sources, we used the catalogue of González-Fernández et al. (2015). Targets were selected on the basis of near-IR photometry from 2MASS, with spectral types confirmed from follow-up optical spectroscopy.

(iii) For targets bright in the mid-IR, we used the catalogues compiled from the *Spitzer* SAGE survey by Bonanos et al. (2009, 2010). Objects were classified on the basis of their mid-IR colours, a technique calibrated by stars in the two MCs with known spectral types from Humphreys (1979a,1979b) and Massey & Olsen (2003).

(iv) In addition to the above, we also used the LMC study of Buchanan et al. (2006) which selected bright 8 μm sources from *Spitzer/IRAC* and classified them on the basis of *Spitzer/IRS* mid-IR spectroscopy. From this catalogue we selected those sources confirmed to belong to the LMC, and which had O-rich signatures in their spectra.

(v) Finally, we took the samples of dusty and/or maser-emitting RSGs from van Loon et al. (2005a), Goldman et al. (2017), and Goldman et al. (2018). These stars are thought to have thick dusty envelopes, and so are often very faint in the optical, but are spectroscopically confirmed RSGs.

For each source in our master data base, we then collate (where available) *UBV* photometry from the Magellanic Clouds Photometric Survey (MCPS; Zaritsky et al. 2002, 2004), *BV* photometry from Massey & Olsen (2003, hereafter M-O03), *I*-band photometry from *DENIS* (Cioni et al. 2000), *JHK* photometry from 2MASS (Skrutskie et al. 2006), and mid-IR photometry from *Spitzer*/IRAC (Meixner et al. 2006; Gordon et al. 2011) and WISE (Wright et al. 2010). To aid in vetting our source list of foreground interlopers, we also search for proper motion measurements from *Hipparcos* (ESA 1997), and radial velocity measurements and luminosity classifications from González-Fernández et al. (2015). Targets are rejected from the catalogue if they have any of the following:

(i) Heliocentric radial velocities v_{hel} less than 70 km s^{-1} below the average for their putative host galaxy, i.e. $v_{hel} < 80$ km s^{-1} and $v_{hel} < 200$ km s^{-1} for the SMC and LMC, respectively, based on the results of González-Fernández et al. (2015).

(ii) Proper motions greater than 1 mas yr^{-1}, from *Hipparcos* (ESA 1997).

(iii) Luminosity classes of II or fainter, based on González-Fernández et al. (2015).

The foreground extinction to each star was determined from the extinction maps of Zaritsky et al. (2002, 2004), which were themselves constructed from the apparent colours of hot stars. For each star in our catalogue, we took the visual extinction A_V to be the median of that at the star's position and the neighbouring 8 pixels (corresponding to a radius of 1 arcmin), with the error taken to be the standard deviation. We then dereddened the star's photometry according to the extinction law in Gordon et al. (2003) appropriate for the star's host galaxy.

2.2 Determining bolometric luminosities

The dereddened photometry was first converted to fluxes using the filter profile information made available by the SVO Filter Profile Service.[2] The spectral energy distributions (SEDs) were resampled on to a logarithmically spaced wavelength axis using the `spline` function in IDL, before being integrated using the IDL function

[1] See also Gordon, Humphreys & Jones (2016) for extragalactic studies of RSGs in M31 and M33.

[2] http://svo2.cab.inta-csic.es/theory/fps/

Downloaded from https://academic.oup.com/mnras/article-abstract/478/3/3138/4999916 by Liverpool John Moores University user on 24 September 2018

int_tabulated to find their apparent bolometric luminosities. Absolute luminosities were determined from the distance moduli of 18.49 and 18.95 for the LMC and SMC, respectively (Pietrzyński et al. 2013; Graczyk et al. 2014). Example plots of SEDs for the brightest sources in each galaxy are shown in Fig. 1.

In our study we have *not* corrected for circumstellar extinction, which is well known to exist around many cool SGs (e.g. Kastner & Weintraub 1998; van Loon et al. 2005a; de Wit et al. 2008). Instead, we have made the assumptions that any flux lost to absorption by circumstellar material is re-radiated in the mid-IR, and that the radiation is isotropic (the latter assumption is discussed further in Section 3.1). For all but a small number of stars in our sample, the contribution to the total luminosity by the flux at our longest wavelength data point (*WISE-4*, 24 μm) is very small. For objects which are bright at 24 μm, we also add in the flux at 70 μm from Jones et al. (2017). Even for the brightest, reddest star in our sample (WOH G64), the flux at wavelengths >24 μm is negligible (see Section 3).

At the opposite end of the spectrum, we have estimated the amount of flux emitted at short wavelengths by creating a blackbody spectrum and matching it to the dereddened *U*- or *B*-band flux. For K and M types, we use a blackbody $T_{\rm eff}$ of 4000 K, for G types 5000 K, unless the object already has a specific $T_{\rm eff}$ estimate in Neugent et al. (2010) or Neugent et al. (2012). The amount of flux emitted at these wavelengths by cool SGs is again small, only a few ×0.01 dex. This contribution rises to ∼0.1 dex for the earliest spectral types in our sample.

A summary of the observational data on the 20 most luminous cool SGs in each galaxy is listed in Table1. Full details on all stars in this work, including all photometry, can be found online at CDS via anonymous ftp to cdsarc.u-strasbg.fr (130.79.128.5) or via http://cdsarc.u-strasbg.fr/viz-bin/qcat?J/MNRAS.

3 LUMINOSITY DISTRIBUTIONS AND $L_{\rm MAX}$

Histograms of the number of stars per luminosity bin for the two MCs are plotted in Fig. 2. In both galaxies, we see what at first look appears to be a sharp cliff-edge to the luminosity distribution, with one more object ∼0.2 dex brighter. There are three possible explanations for this edge: there is a genuine hard upper limit to the luminosities of cool SGs; the lifetime of the cool SG phase at high luminosities is very short; or it is caused by small number statistics at the upper end of the initial mass function. In the following sections we will argue that this cut-off is *not* an artefact of low number statistics. Though we cannot distinguish between a hard upper limit to *L* and very short cool SG lifetimes above this limit, we will show that there is a genuine tension with evolutionary theory, particularly in the case of the SMC.

3.1 Comparisons between the LMC and SMC

In the LMC, we see that there is an apparent truncation of the luminosity distribution at $\log(L/{\rm L}_\odot) = 5.5$. If we were to extrapolate beyond this limit at the gradient seen at $\log(L/{\rm L}_\odot) > 5$, we would expect to see ≈4 stars above $\log(L/{\rm L}_\odot) = 5.5$, whereas we see only one. This bright star is WOH G64, with $\log(L/{\rm L}_\odot) = 5.77$. At this luminosity, stellar evolutionary models imply an initial mass of $\gtrsim$40 M$_\odot$, and an age of $\lesssim$5Myr. Despite this young age, the star seems to be relatively isolated, with the closest markers of recent star formation such as ionized nebulae or other massive stars over 70 arcsec away (Levesque et al. 2009). Further, this object is highly variable, with minimum-to-maximum variability ranging from 3 mag at *B* to 1.5 mag at *I* (MACHO; Soszyński et al. 2009). Further, the variability in the different wavebands appears to be positively correlated, implying a variable $L_{\rm bol}$ rather than in just colour. Finally, we note that several authors have studied the SED of WOH G64 and concluded that the circumstellar material cannot be spherically symmetric (Roche, Aitken & Smith 1993; van Loon et al. 1999; Ohnaka et al. 2008; Goldman et al. 2017). In particular, Ohnaka et al. modelled the excess emission as originating in a dusty torus, which resulted in the star's luminosity being revised downwards to $\log(L/{\rm L}_\odot) = 5.45$, which would imply a much lower initial mass of around 25 M$_\odot$. Excluding WOH G64, the five next most luminous stars cluster around $5.4 < \log(L/{\rm L}_\odot) < 5.5$, suggesting an upper luminosity limit for the LMC of $\log(L/{\rm L}_\odot) = 5.5$.

In the SMC (Fig. 2, right-hand panel), the cliff-edge to the luminosity distribution occurs at a lower *L*, $\log(L/{\rm L}_\odot)= 5.36$. Again, from a simple extrapolation to higher luminosities we would expect to see ≈7 stars above this limit, rather than just the one star observed. The bright star is Dachs SMC 1-4, an RSG with a luminosity of $\log(L/{\rm L}_\odot) = 5.55$. Unlike WOH G64, this star is only moderately variable, with a minimum-to-maximum amplitude of 0.25 mag in *R* (Pojmański 2002). It is therefore less easy to discount Dachs SMC 1-4, and so it may indeed be a representative of $L_{\rm max}$ in the SMC.

In each galaxy, we conservatively estimate the observed upper luminosity limit as being that of the second and third brightest stars, so as to insulate our conclusions from outliers and peculiar objects. Under this definition, the upper luminosity limits $L_{\rm max}$ for the two galaxies are $\log(L/{\rm L}_\odot)$= 5.4 and 5.5 for the SMC and LMC, respectively. Before proceeding to study the predictions of stellar evolution models in detail, we first note that this behaviour of $L_{\rm max}$ with metallicity goes opposite to the direction one would naively expect. At lower metallicity, mass-loss rates on the MS should be lower, and so post-MS envelope masses should be higher. This would allow stars with higher masses to evolve to the RSG stage in lower metallicity environments. However, we see the opposite: $L_{\rm max}$ is higher in the LMC, where the metallicity is roughly twice that of the SMC (Davies et al. 2015).

To investigate whether the above result is an artefact of number statistics, we perform a simple numerical experiment in which we model the SMC simply as a scaled-down version of the LMC.[3] We take the luminosities of the stars in the LMC, and randomly select a fraction of those values to reflect the smaller sample size of the SMC. We then determine the most likely value of $L_{\rm max}$ from this reduced sample, as well as the number of stars with $\log(L/{\rm L}_\odot) > 5.4$, $N_{5.4}$. We repeat this experiment 10^5 times to determine the probability distributions of each of these quantities. We find that, if the two galaxies had the same intrinsic luminosity distribution, in the SMC we would expect an average $L_{\rm max}= 5.52^{+0.05}_{-0.04}$, with $N_{5.4} = 2.6^{+1.4}_{-1.6}$ (67 per cent confidence limits). The probability of finding only one star with a luminosity above $\log(L/{\rm L}_\odot) = 5.4$ is 19 per cent, while the probability of zero stars above this limit is 4 per cent. Therefore, though not conclusive, the balance of probability suggests that $L_{\rm max}$ is lower in the SMC than in the LMC, a result which is the opposite to that predicted by evolutionary models. This is broadly in agreement with Humphreys (1983), who found that the most luminous cool stars in their LMC and SMC samples were roughly the same,

[3]The current star formation rate of the SMC is ∼6 times lower than the LMC (Kennicutt et al. 2008), so their similar cool SG populations support a significantly higher ratio of cool to blue SG in the former, as previously discussed by Langer & Maeder (1995).

Downloaded from https://academic.oup.com/mnras/article-abstract/478/3/3138/4999916 by Liverpool John Moores University user on 24 September 2018

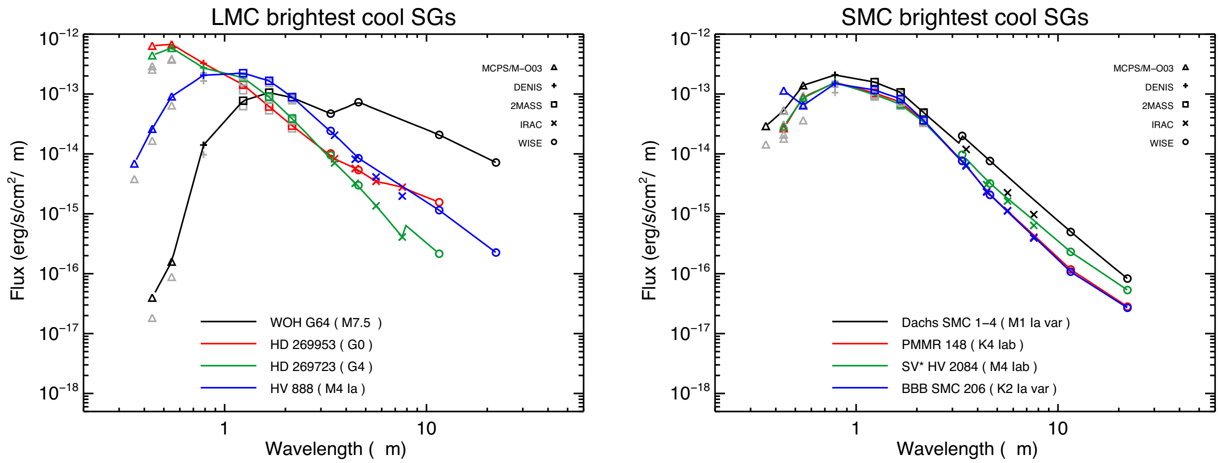

Figure 1. Observed spectral energy distributions of the three most luminous stars in each galaxy. The different symbols indicate the source of the photometry, as described by the legend in the upper left of each panel. The grey symbols show the photometry prior to correction for reddening.

notwithstanding their selective samples and the issues that will be discussed in Section 3.2.

Looking at the whole of the high-end of the luminosity distribution below L_{max}, we can say that the evidence for the two galaxies having different intrinsic luminosity distributions is weak. A Kolmogorov–Smirnov test of the cumulative luminosity distributions for all stars with $5.0 < \log(L/L_{\odot}) < 5.4$ shows that there is a 60 per cent probability that the luminosities of the cool SGs in each galaxy are drawn from the same parent distribution.

3.2 Comparisons with previous work

Our findings for L_{max} are substantially lower than $\log(L/L_{\odot}) =$ 5.7–5.9 originally claimed in Humphreys & Davidson (1979), later revised to $\log(L/L_{\odot}) = 5.66$ by Humphreys (1983) and Elias et al. (1985). This is due in large part to a systematic downward revision of the luminosities of the cool SGs in these galaxies. On average, we find luminosities that are 0.17 dex fainter than those listed in table 15 of Elias et al. The explanation for this is threefold; first, we are using a slightly lower distance modulus to the LMC (18.49, compared with 18.6 in Humphreys 1979a and Elias et al.). Secondly, improvements in infrared photometry (higher sensitivity and spatial resolution, especially at longer wavelengths) mean that we can obtain reliable SEDs for all stars in our sample, without relying on uncertain bolometric corrections derived from a subset of our sample. Thirdly, our treatment of extinction is fundamentally different to that of Elias et al. These authors inferred the total (interstellar + circumstellar) extinction by comparing the stars' colours to 'intrinsic' colours of stars of the same spectral type. They did this by assuming that stars of the same spectral type have the same intrinsic $B - V$, regardless of metallicity, and used Galactic stars as templates. This involves dereddening the Galactic stars, again accounting for both inter and circumstellar extinction, which as Elias et al. themselves point out is extremely problematic. By contrast, we have used extinction maps to infer the foreground (interstellar) extinction, and assumed that the luminosity integrated between the U band and 24µm is independent of circumstellar extinction.

One caveat to our treatment of extinction is that the circumstellar dust could be clumpy, which would reduce the extinction per unit infrared excess. However, this would cause us to overestimate the luminosity, further reducing L_{max}, and increasing the disagreement with Elias et al. (1985). Further, it is unlikely that large amounts of cool dust, which emits at longer wavelengths than 24µm, are causing us to underestimate the luminosities of the stars in our sample. For all but a handful of stars the flux at 24 µm is already negligible compared to that emitted at shorter wavelengths. For the star with the largest IR excess, WOH G64 in the LMC, we have added in the 70 µm *Spitzer*/MIPS photometry (Jones et al. 2017) to account for the contribution from cool dust. Even in this extreme case, the flux emitted between 24 and 70µm contributes only 0.05 dex to the bolometric luminosity.

We can also compare to other estimates of the brightest cool SGs in the MCs. Massey et al. (2009, hereafter M09) revisited the luminosities of the RSGs in the LMC and SMC derived in L06, obtaining values of L_{bol} using both V-band and K-band photometry in conjunction with their bolometric corrections measured from MARCS model atmospheres. It was noted by M09 that the luminosities determined from the V band were systematically higher than those determined at K, by an average of 0.12 dex. For the stars we have in common with M09 we find good agreement between their K-based luminosities and our L_{bol}s. Therefore, we also reproduce the result that M09's V-band luminosities are brighter by ∼0.1 dex. The explanation for this is compound. First, the atmospheric models used by M09 (and references therein) are known to systematically overestimate the strengths of the TiO absorption bands at a given effective temperature T_{eff} (Davies et al. 2013). This causes the total (foreground plus circumstellar) extinction and the T_{eff} to both be underestimated. This means that, for a *dereddened* V-band flux, one will overestimate the star's luminosity. Though the bolometric corrections in L06 seem consistent with ours (see Appendix), they are for *dereddened* V-band fluxes – that is, the foreground *and* circumstellar extinction must first be accounted for. By contrast, our BCs already take into account the average circumstellar extinction at a given spectral type, and so only knowledge of the foreground extinction is required.

3.3 Statistical completeness

To assess the completeness of our samples of cool SGs in the MCs, in Fig. 3 we replot the luminosity distributions for each galaxy illustrating the contributions of the individual samples used in our study. The red bars in the figures show the luminosities of the objects in the Bonanos studies (Bonanos et al. 2009, 2010), while the yellow bars show those from González-Fernández et al. (2015) which were

Downloaded from https://academic.oup.com/mnras/article-abstract/478/3/3138/4999916 by Liverpool John Moores University user on 24 September 2018

Table 1. Name, position, luminosity, and extinction of the 20 most luminous cool SGs in each of the LMC and SMC. In this table we provide for each star the SIMBAD designation, as well as those from Massey (2002) and González-Fernández et al. (2015) where available. Where stars are known to be variable, we list the minimum and maximum known spectral types and luminosity classes. Full observational information on all stars in this study (over 300 per galaxy), including photometry from the U band to 70μm, is available electronically at the CDS via anonymous ftp to cdsarc.u-strasbg.fr (130.79.128.5) or via http://cdsarc.u-strasbg.fr/viz-bin/qcat?J/MNRAS.

SIMBAD Name	[M2002]	[GDN2015]	Spec Type	RA DEC (J2000)	$\log(L/L_\odot)$	A_V
LMC						
WOH G064	–	–	M7.5	04 55 10.48 −68 20 29.8	5.77 ± 0.04	0.72 ± 0.12
HD 269953	–	–	G0	05 40 12.18 −69 40 05.0	5.50 ± 0.04	0.72 ± 0.15
HD 269723	–	–	G4	05 32 24.96 −67 41 53.7	5.48 ± 0.08	0.51 ± 0.34
HV 888	–	–	M4 Ia	05 04 14.14 −67 16 14.4	5.48 ± 0.04	0.42 ± 0.19
SV∗ HV 2450	–	–	M2 Ia	05 19 53.26 −68 04 03.8	5.45 ± 0.04	0.58 ± 0.18
SP77 46-44	LMC 145013	–	M2.5 Ia-Ib	05 29 42.21 −68 57 17.4	5.40 ± 0.02	0.12 ± 0.08
SV∗ HV 5618	LMC 071357	–	M1 I	05 07 05.66 −70 32 44.0	5.38 ± 0.04	0.32 ± 0.21
SP77 31-16	–	–	–	04 54 36.84 −69 20 22.1	5.35 ± 0.03	0.56 ± 0.15
LI-LMC 1100	–	–	–	05 27 40.78 −69 08 05.7	5.34 ± 0.00	0.50 ± 0.10
[MG73] 46	–	–	–	05 35 55.23 −69 09 59.5	5.34 ± 0.04	1.10 ± 0.21
[M2002] LMC 165543	LMC 165543	–	G1 Ia	05 36 26.79 −69 23 51.4	5.33 ± 0.04	0.49 ± 0.19
[GDN2015] LMC252	–	LMC252	M0 Ia-Ib	05 39 32.34 −69 34 50.1	5.30 ± 0.04	0.89 ± 0.24
[M2002] LMC 144217	LMC 144217	–	M3 Ia	05 29 27.58 −69 08 50.3	5.30 ± 0.03	0.51 ± 0.14
HV 2561	LMC 141430	–	M2 Ia	05 28 28.86 −68 07 07.9	5.29 ± 0.05	0.76 ± 0.27
[M2002] LMC 136042	LMC 136042	–	M4 Ia-Ib	05 26 34.80 −68 51 40.0	5.27 ± 0.03	0.34 ± 0.16
HV 916	–	–	M3 Ia	05 14 49.72 −67 27 19.7	5.27 ± 0.04	0.76 ± 0.23
[GDN2015] LMC45	–	LMC45	M3 Ia	05 26 23.54 −69 52 25.8	5.27 ± 0.04	0.22 ± 0.16
LI-LMC 183	LMC 023095	–	M2	04 55 03.07 −69 29 12.8	5.24 ± 0.03	0.49 ± 0.18
SV∗ HV 2595	LMC 147199	–	M4 I	05 30 20.94 −67 20 05.4	5.23 ± 0.03	0.30 ± 0.16
WOH S 229	LMC 113364	–	M1 I	05 19 03.26 −69 39 55.3	5.23 ± 0.03	0.42 ± 0.12
SMC						
Dachs SMC 1-4	SMC 018592	–	M0.5-M3 Ia-Ib	00 51 03.86 −72 43 17.6	5.55 ± 0.01	0.48 ± 0.05
PMMR 148	SMC 056389	–	K4 Iab	01 03 27.64 −72 52 09.6	5.39 ± 0.03	0.36 ± 0.14
SV∗ HV 2084	SMC 069886	SMC400	M4 Iab	01 09 38.24 −73 20 02.4	5.35 ± 0.02	0.28 ± 0.09
[GDN2015] SMC354	–	SMC354	G1 Ib	01 03 53.87 −72 45 15.0	5.34 ± 0.05	0.53 ± 0.21
PMMR 37	SMC 018136	–	K4.5 Ia-Ib	00 50 56.09 −72 15 06.1	5.33 ± 0.03	0.36 ± 0.14
LHA 115-S 30	SMC 049478	–	K5 Ia-Ib	01 00 41.51 −72 10 37.1	5.27 ± 0.04	0.40 ± 0.18
SV∗ HV 11423	SMC 050028	–	M0Iab	01 00 55.20 −71 37 52.9	5.25 ± 0.02	0.27 ± 0.11
BBB SMC 206	SMC 010889	–	K2-K5 Ia-Ib	00 48 27.02 −73 12 12.3	5.25 ± 0.02	0.70 ± 0.07
SV∗ HV 1475	SMC 013472	–	G5.5-M0 Ia-Ib	00 49 24.55 −73 18 13.6	5.24 ± 0.02	0.59 ± 0.09
Dachs SMC 2-37	SMC 059803	–	G7-K3 Ia-Ib	01 04 38.21 −72 01 27.0	5.24 ± 0.03	0.27 ± 0.18
PMMR 9	SMC 005092	–	M1.5 Ia-Ib	00 45 04.57 −73 05 27.7	5.23 ± 0.03	0.79 ± 0.13
[M2002] SMC 64663	SMC 064663	–	G6-K3.5 Ia-Ib	01 06 47.67 −72 16 11.8	5.21 ± 0.03	0.42 ± 0.15
PMMR 52	SMC 025888	–	K3.5 Ia-Ib	00 53 09.12 −73 04 03.8	5.21 ± 0.02	0.46 ± 0.05
LIN 235	–	–	K1-K4 Ia-Ib	00 53 08.95 −72 29 38.6	5.20 ± 0.02	0.54 ± 0.10
BBB SMC 138	SMC 012322	–	K3-M1.5 Ia-Ib	00 49 00.35 −72 59 35.9	5.19 ± 0.03	0.72 ± 0.14
PMMR 70	SMC 030616	–	K0-K2.5 Ia-Ib	00 54 35.90 −72 34 14.4	5.18 ± 0.02	0.54 ± 0.11
PMMR 41	SMC 020133	–	K3-M1.5 Ia-Ib	00 51 29.68 −73 10 44.2	5.18 ± 0.02	0.54 ± 0.08
[GDN2015] SMC54	–	SMC54	–	00 42 17.14 −74 06 15.3	5.16 ± 0.08	0.18 ± 0.38
PMMR 62	–	–	K3-M1.5 Ia-Ib	00 53 47.94 −72 02 09.5	5.16 ± 0.05	0.34 ± 0.22
PMMR 105	SMC 047757	–	K0 Ia-Ib	01 00 00.58 −72 19 40.4	5.14 ± 0.02	0.45 ± 0.08

not found in Bonanos. The subsequent colours, as shown in the legends, indicate the stars found in the corresponding survey that were not present in the other surveys listed above it in the legend.

We see that almost all stars are found in the IR-based surveys of González-Fernández et al. (2015), Bonanos et al. (2009, 2010), and Neugent et al. (2010, 2012). The samples of dust-enshrouded stars (van Loon et al. 2005a; Buchanan et al. 2006; Goldman et al. 2017, 2018) pick up a small number of luminous stars not detected in the IR surveys due to circumstellar extinction. All but a handful of stars from the selective survey of Elias et al. (1985, and references therein) are found in the systematic surveys listed earlier.

The one object known to be luminous but not picked up in our catalogue search is IRAS 05280-6910. This object is part of the dense cluster NGC 1984, and is not well resolved from the other stars in its parent cluster. This object was manually added in to our data base, employing the high spatial resolution photometry of van Loon, Marshall & Zijlstra (2005b).

From these results, we conclude that we are complete at high luminosities ($\log(L/L_\odot) \gtrsim 5.0$). Though the statistical completeness may begin to be non-negligible below this limit, this does not pose a problem for this current work since we are interested primarily in $L_{\rm max}$.

3.4 Comparison with WR stars

Since $L_{\rm max}$ is thought to correspond to the initial mass at which single stars evolve directly from the MS to the WR phase, in Fig. 4 we compare the cool SG luminosity distributions to those of nitrogen-rich WR (WN) stars. We choose to compare to WN stars as these are thought to be the least chemically evolved (Crowther 2007).

Downloaded from https://academic.oup.com/mnras/article-abstract/478/3/3138/4999916 by Liverpool John Moores University user on 24 September 2018

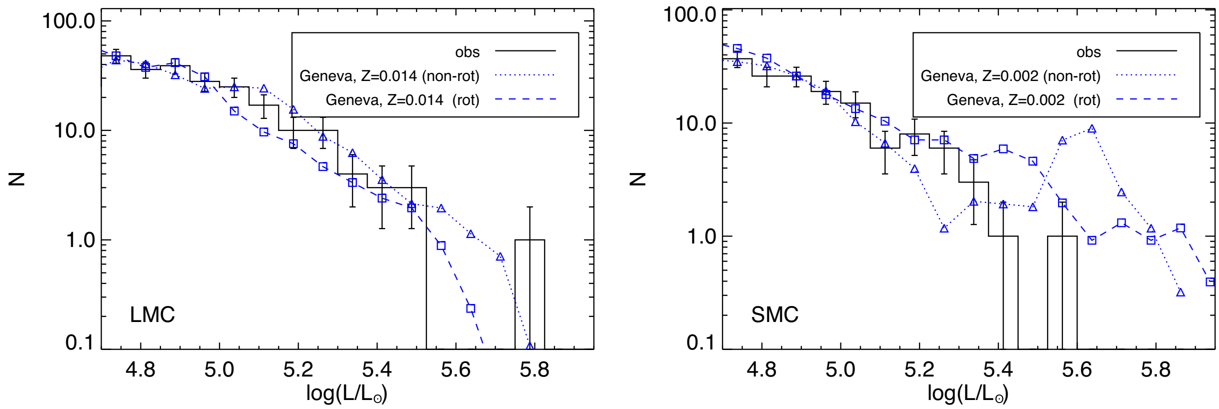

Figure 2. Luminosity distributions for the LMC (left) and SMC (right). Overplotted are the Geneva model predictions for Solar (Ekström et al. 2012) and SMC-like (Georgy et al. 2013). The model predictions have been normalized to fit the observations at log (L/L$_\odot$) = 4.7–5.2.

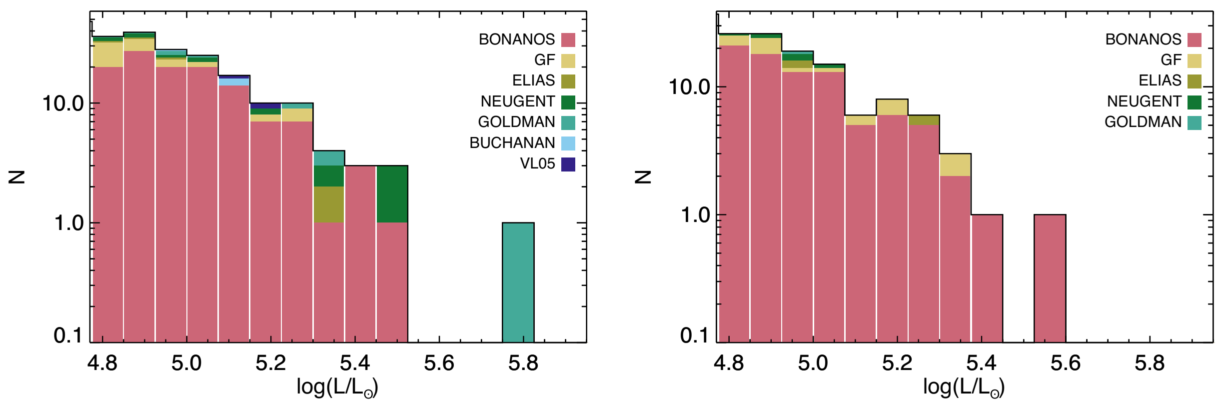

Figure 3. Luminosity distributions for the LMC (left) and SMC (right), illustrating the contributions from the different samples included in this study.

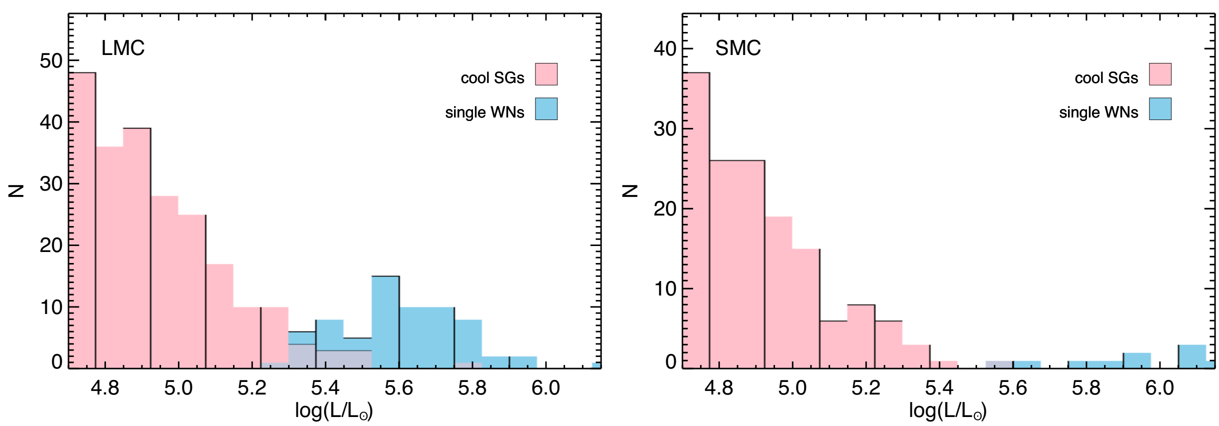

Figure 4. Comparison of the luminosity distributions of RSGs and single WN stars in the two MCs.

For our sample of WNs, we have taken objects from Hainich et al. (2014, 2015), Neugent et al. (2017), and Shenar et al. (2016), and discarded objects that were in known binaries in order to compare only those objects which result from single-star evolution. As a caveat however, we note that we are unable to rule out that some stars in this sample may still have experienced interaction with a companion which is no longer visible (either due to a merger or supernova).

In the LMC (left-hand panel of Fig. 4), the luminosity distributions splice together with a small overlap region between log (L/L$_\odot$) = 5.2–5.5 where presumably stars can experience a shortened cool SG phase before becoming a WR. In the SMC, there is no overlap between the two classifications of star, though this could easily be a result of lower number statistics.

The results presented in Fig. 4 are a clear demonstration of the commonly held view that the evolution of a single star to the WR

Downloaded from https://academic.oup.com/mnras/article-abstract/478/3/3138/4999916 by Liverpool John Moores University user on 24 September 2018

phase requires an initial mass above a certain threshold. This threshold roughly corresponds to the most massive cool SGs, with an overlap region where stars may possibly experience both a cool SG and WR phase (see also van Loon 2017). Under the reasonable assumption that stars which evolve from the cool SG phase to the WR phase do so at ∼constant luminosity, the plot also indicates that the highest luminosity of a cool SG which will explode in that phase is $\log(L/L_\odot) \approx 5.2$–5.3, i.e. the luminosity at which cool SGs and WRs co-exist. This is in agreement with the results of Davies & Beasor (2018), who showed that, of all SNe with pre-explosion detections of the progenitor, the brightest (SN2009hd) had a pre-SN luminosity of $\log(L/L_\odot) = 5.24 \pm 0.08$.

3.5 Comparison to evolutionary models

To make a quantitative comparison between our results and the expectations from evolutionary models, we perform a simple population synthesis analysis. We first generate a population of stars with masses drawn from a Salpeter initial mass function (IMF; Salpeter 1955) and with ages sampled from a uniform random distribution between 0 and 50 Myr, the latter being the expected lifetime of an $8\,M_\odot$ star. For each simulated star we interpolate an evolutionary track at that mass to determine its L and effective temperature $T_{\rm eff}$ at that star's age. If the age is greater than the star's lifetime, or the star is not in the cool SG region of the H–R diagram (i.e. $T_{\rm eff} > 7000$ K) then that star is discarded. To compare to our observations, we construct simulated luminosity distributions (LDs) with the same binning as the observed data, and renormalize the simulations to minimize the differences between the model and observed distributions in the range $4.7 \leq \log(L/L_\odot) \leq 5.2$. We choose this luminosity range as here we expect to be largely complete while also having $\gtrsim$5 stars per bin.[4]

The comparisons of the simulated and observed LDs are shown in Fig. 2, the model predictions overplotted in blue. The models we have chosen are those of the Geneva group, who have published rotating and non-rotating models at Solar and SMC-like metallicity. At lower luminosities ($\log(L/L_\odot) \lesssim 5.3$), the slopes of the observed and simulated LDs match reasonably well, implying that the models correctly reproduce the relative numbers of cool SGs as a function of luminosity. The slope of this part of the LD is a combination of that of the IMF, the mass–luminosity relation for cool SGs (which may not be unique for a given mass), the mass–lifetime relation, and the fraction of this time that a star spends in the cool SG phase. Most evolutionary models agree that the ratio of the post-MS to MS lifetimes is ∼0.08–0.12, being at the lower end of this range for more massive stars, so one would not expect this to be a major source of uncertainty. Therefore, assuming that star formation in the MCs follows the standard Salpeter IMF, the similarity between the simulated and observed LD slopes indicates that the models are correctly predicting the convolution of the mass–luminosity relation and the cool SG lifetimes, at least in a relative sense[5]. Further, the result that the LDs look so similar between the two galaxies implies that this product is not strongly affected by metallicity.

[4]If we are incomplete in this range, this would require the simulated LD to be moved upwards in number, which would also cause an increase in the simulated $L_{\rm max}$.

[5]We note that we have made no attempt here to reproduce the absolute LDs of each galaxy by, e.g. benchmarking against their global star formation rates.

The discrepancy between the models and the observations comes when we look at the highest luminosities. In the LMC (left-hand panel of Fig. 2) the Solar metallicity models provide a very good match to the observed LD: at $\log(L/L_\odot) \gtrsim 5.6$, we see a decrease in the fraction of time spent by stars in the cool SG phase. This causes a downturn in the predicted LD, fitting the observed $L_{\rm max}$ to within the errors. However, models with an LMC-like metallicity (not available at the time of writing) would have a larger $L_{\rm max}$, owing to the reduced mass-loss rates on the MS as discussed earlier. The effect is more pronounced when we look at the SMC (right-hand panel of Fig. 2). Both the rotating and non-rotating models predict that we should be seeing cool SGs with luminosities of $\log(L/L_\odot) = 5.7$–5.8. Quantitatively, we see only one star in the SMC with a luminosity above $\log(L/L_\odot) \geq 5.36$, compared to 25 (18) predicted by rotating (non-rotating) models.[6] This implies that, at higher luminosities, either stars cannot evolve to the cool SG phase *or* this phase is so short that it is unlikely to be observable. In either case, this result implies that the latest population synthesis models (e.g. Leitherer et al. 2014) are underestimating the ionizing fluxes and producing integrated colours that are too red for populations at low metallicity.

3.6 Possible causes of a reduced $L_{\rm max}$

Having argued in the previous section that single-star models substantially overpredict the numbers of high-luminosity cool SGs, we now discuss various potential solutions to this discrepancy. For the purposes of this discussion we characterize this discrepancy in terms of the apparent $L_{\rm max}$, which is the brightest cool SG that one is likely to detect in a finite population of stars.

The first obvious aspect to discuss is that of stellar winds. It is commonly argued that the upper luminosity limit for RSGs is a result of higher mass stars having stronger winds, losing a larger fraction of their initial mass during their lifetimes. Above some mass, almost all the H-rich portion of envelope is lost prior to the RSG phase, keeping the star in the blue. Hence, increasing the mass-loss rate $\dot{M}$ would in turn reduce the observed $L_{\rm max}$.

On the main sequence, the mass-loss rate prescriptions of O stars employed in the Geneva models seem to be supported by observations (Mokiem et al. 2007), and so there is little justification in increasing these. Further, we have shown here that $L_{\rm max}$ does *not* increase with decreasing metallicity, as one would expect if line-driven winds were the cause. This suggests that, if stellar winds govern the observed value of $L_{\rm max}$, then these winds would have to be metallicity-independent continuum-driven winds, such as those suggested for LBVs (e.g. Smith & Owocki 2006).

In terms of mass-loss during the cool SG phase, increasing $\dot{M}$ for RSGs seems poorly justified. Indeed, measurements of how $\dot{M}$ evolves throughout the RSG phase suggest that all evolutionary models are currently *overestimating* the total integrated mass lost during this time, at least for stars with initial masses $\sim 16\,M_\odot$ (Beasor & Davies 2018). This would result in the opposite of what we see in the MCs: it would make higher mass single stars more likely to explode in the RSG phase, moving $L_{\rm max}$ to higher luminosities. One way out of this would be if stars experience a short period of enhanced mass-loss towards the end of the RSG phase which is so brief that only a few stars per galaxy would be in this phase at any one time. Such stars may appear as OH/IR stars, characterized by large infrared excesses and circumstellar maser emission.

[6]We note that rotational velocities as high as those of the rotating Geneva models are rarely seen in the LMC (Ramírez-Agudelo et al. 2013).

Downloaded from https://academic.oup.com/mnras/article-abstract/478/3/3138/4999916 by Liverpool John Moores University user on 24 September 2018

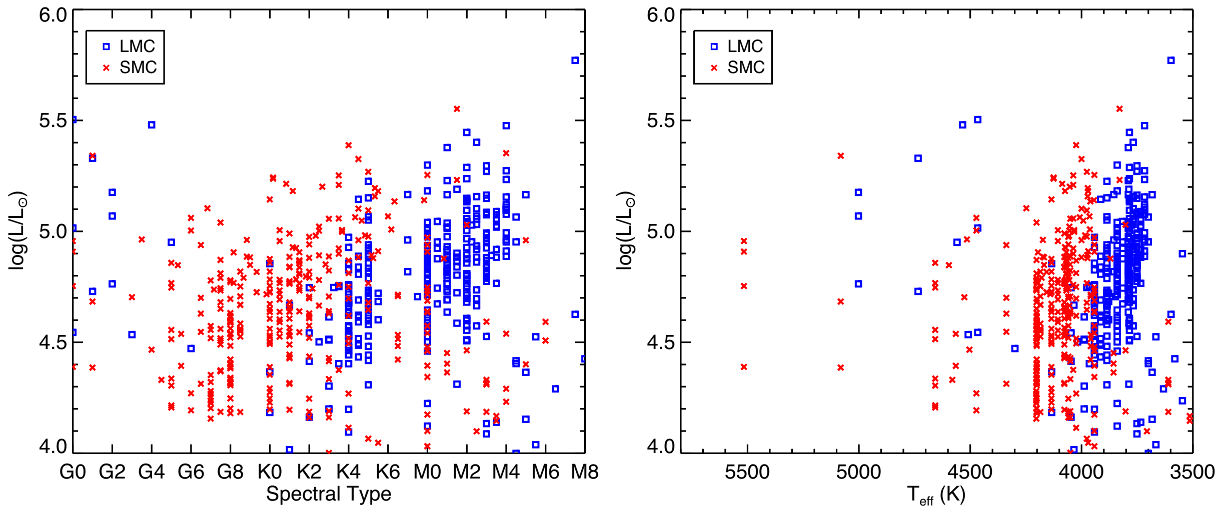

Figure 5. *Left:* Observational H–R diagram for the cool SGs in each galaxy. *Right:* Same as the left-hand panel, but with spectral types converted to effective temperatures using the temperature scales of Tabernero et al. (2018).

If we concentrate on the LMC, there are four out of 73 stars in our sample which have OH masers with luminosities $\log(L/L_\odot) \geq 5.0$ (above which we consider our sample to be complete). If all RSGs experience an OH/IR phase, for a canonical RSG lifetime of 10^6yr this suggests an OH/IR lifetime of a few $\times$ 10^4yr. With a typical mass-loss rate of $\sim 10^{-4}\,M_\odot\,yr^{-1}$ (e.g. Goldman et al. 2017), there is the potential to lose several Solar masses of envelope during this phase, an amount which would dwarf that lost to this point.

One other way to reduce L_{max} would be to invoke the effects of binary mass transfer as a way to increase the amount of mass lost during a star's life. Specifically, a trend of increasing the interacting binary fraction with initial stellar mass would have the effect of reducing the probability of forming cool SGs at high luminosities. Moe & Di Stefano (2017) argue that the single-star fraction decreases as a function of initial stellar mass, while the companion frequency at short periods increases. Together, these effects would serve to decrease the likelihood of a primary becoming a cool SG at higher initial masses.

Quantitative modelling of the luminosity distribution of cool SGs for a population of stars would need to account for the IMF and star formation rate, as well as the mass-dependence of the lifetimes of the MS and post-MS phases, the luminosity evolution within the cool SG phase, and the binary fractions and period distributions. Such a work is beyond the scope of this study and will be the subject of a future paper.

3.7 Observational H–R diagram

To compare the differences in the cool SG populations of the two MCs, in Fig. 5 we plot an observational H–R diagram of all stars in our two samples. In the left-hand panel we plot spectral type on the horizontal axis; on the right we plot the same but employing the temperature scale of Tabernero et al. (2018). Though incompleteness effects are obvious below $\log(L/L_\odot) \lesssim 4.7$, one can clearly see that there is an offset in spectral types between the two galaxies.

The shift to earlier average spectral types of RSGs from early-M to late-K as one moves from the LMC to the SMC is well known (e.g. Humphreys 1979b; Elias et al. 1985). Up until recently there has been little compelling evidence as to whether this represents a shift of the Hayashi limit to higher T_{eff} at lower metallicity, or whether it is simply an effect of lower metal abundances reducing the strengths of the TiO absorption lines which define the transition from K to M types (Davies et al. 2013). However, what Fig. 5 shows is that the systematic shift to earlier spectral types in the SMC compared with the LMC goes beyond a shift from M to K, but also reaches to late-G types. There are very few cool SGs in the LMC with spectral types earlier than K2. By contrast, there are many cool SGs in the SMC with spectral types earlier than K. This *cannot* be explained as a metallicity effect alone, as the differences between G and K classifications are driven mainly by ionization rather than simply strengths of lines. This difference must then be caused by a metallicity dependence of (a) the temperature of the Hayashi limit, and/or (b) the speed at which SGs cross the H–R diagram, either on their way *to* or back *from* the RSG phase. Interestingly, there *are* stars in the SMC which have late spectral types (>M2), particularly at lower luminosities. Many of these objects could be super-AGB stars, the descendants of intermediate-mass stars.

In the right-hand panel of Fig. 5 we convert the spectral types of the stars to effective temperature using the calibration of Tabernero et al. (2018), based on comparisons to LTE model atmospheres. We have many stars in common with Tabernero et al., which is based on the González-Fernández et al. (2015) sample, though our sample has a higher level of completeness particularly for objects with large reddening. Predictably, our results show the same as Tabernero et al., specifically that the LMC stars are systematically cooler than those in the SMC. We note that in the Tabernero scale, the dispersion in T_{eff} at a given spectral type is quite large, up to ± 100 K, with a 200 K spread being as large as the T_{eff} difference between e.g. K2 and M1 spectral types. This explains the apparent paradox whereby no temperature scale was detected by Davies et al. (2015) yet object-by-object comparisons with Tabernero et al. showed good agreement; the Davies et al. sample of $\sim$10 objects per galaxy was too small to detect the subtle variations in T_{eff} as a function of spectral type.

4 CONCLUSIONS

We have combined various surveys of cool SGs and used multi-wavelength survey photometry from the *U* band to the mid-infrared to redetermine the luminosity distributions of cool massive stars in

Downloaded from https://academic.oup.com/mnras/article-abstract/478/3/3138/4999916 by Liverpool John Moores University user on 24 September 2018

the Large and Small Magellanic Clouds. Our main findings are as follows:

(i) The most luminous cool stars in the LMC and SMC have $\log(L/L_\odot) = 5.77$ and 5.55, respectively, though the brightest of these is highly variable. The next most luminous stars have $\log(L/L_\odot) = 5.50$ and 5.36, respectively. If these stars represent the upper luminosity limit $L_{\rm max}$ (otherwise known as the H–D limit), this is a downward revision of the previously quoted limit of $\log(L/L_\odot) \simeq 5.7$ in the literature.

(ii) We find no evidence to support the commonly held view that $L_{\rm max}$ is higher at lower metallicity. Indeed our results indicate that it is unlikely that $L_{\rm max}$ in the SMC is higher than in the LMC, even after accounting for low number statistics. This argues against metallicity-dependent mass-loss being the cause of $L_{\rm max}$.

(iii) A population synthesis analysis of the two luminosity distributions reveals that the Geneva evolutionary models predict too many luminous cool stars, particularly in the SMC. Specifically, models predict >19 cool SGs in the SMC with luminosities $\log(L/L_\odot) > 5.36$, whereas we see only one.

(iv) The luminosity distributions of cool SGs splice together with those of apparently single WR stars in each of the MCs, suggesting a changing evolutionary sequence of massive stars with increasing initial mass.

(v) The spectral types of cool SGs are earlier in the SMC than in the LMC, a well-known result. However, the shift extends beyond that of M to K, with a substantial number of G SGs in the SMC. This implies that the average temperatures of cool SGs are hotter at lower metallicities.

ACKNOWLEDGEMENTS

The authors would like to thank the referee Jacco van Loon for suggestions and comments which helped us improve the paper, Fabian Schneider for enquiring about the upper luminosity of cool SGs in the LMC, and Nathan Smith for useful comments and discussion. This publication makes use of data products from the Wide-field Infrared Survey Explorer, which is a joint project of the University of California, Los Angeles, and the Jet Propulsion Laboratory/California Institute of Technology, funded by the National Aeronautics and Space Administration. This publication makes use of data products from the Two Micron All Sky Survey, which is a joint project of the University of Massachusetts and the Infrared Processing and Analysis Center/California Institute of Technology, funded by the National Aeronautics and Space Administration and the National Science Foundation. This work made use of the IDL astronomy library, available at https://idlastro.gsfc.nasa.gov, and the Coyote IDL graphics library.

REFERENCES

Beasor E. R., Davies B., 2018, MNRAS, 475, 55
Bonanos A. Z. et al., 2009, AJ, 138, 1003
Bonanos A. Z. et al., 2010, AJ, 140, 416
Buchanan C. L., Kastner J. H., Forrest W. J., Hrivnak B. J., Sahai R., Egan M., Frank A., Barnbaum C., 2006, AJ, 132, 1890
Chiosi C., Maeder A., 1986, ARA&A, 24, 329
Cioni M.-R. et al., 2000, A&AS, 144, 235
Crowther P. A., 2007, ARA&A, 45, 177
Davies B. et al., 2013, ApJ, 767, 3
Davies B., Beasor E. R., 2018, MNRAS, 474, 2116
Davies B., Kudritzki R.-P., Gazak Z., Plez B., Bergemann M., Evans C., Patrick L., 2015, ApJ, 806, 21
de Wit W. J. et al., 2008, ApJ, 685, L75
Ekström S. et al., 2012, A&A, 537, A146
Elias J. H., Frogel J. A., Humphreys R. M., 1985, ApJS, 57, 91
ESA, 1997, The Hipparcos and Tycho Catalogues. Astrometric and Photometric Star Catalogues Derived from the ESA HIPPARCOS Space Astrometry Mission ESA SP -1200
Georgy C. et al., 2013, A&A, 558, A103
Goldman S. R. et al., 2017, MNRAS, 465, 403
Goldman S. R. et al., 2018, MNRAS, 473, 3835
González-Fernández C., Dorda R., Negueruela I., Marco A., 2015, A&A, 578, A3
Gordon K. D. et al., 2011, AJ, 142, 102
Gordon K. D., Clayton G. C., Misselt K. A., Landolt A. U., Wolff M. J., 2003, ApJ, 594, 279
Gordon M. S., Humphreys R. M., Jones T. J., 2016, ApJ, 825, 50
Graczyk D. et al., 2014, ApJ, 780, 59
Hainich R. et al., 2014, A&A, 565, A27
Hainich R., Pasemann D., Todt H., Shenar T., Sander A., Hamann W.-R., 2015, A&A, 581, A21
Humphreys R. M., 1979a, ApJS, 39, 389
Humphreys R. M., 1979b, ApJ, 231, 384
Humphreys R. M., 1983, ApJ, 265, 176
Humphreys R. M., Davidson K., 1979, ApJ, 232, 409
Jones O. C. et al., 2017, MNRAS, 470, 3250
Kastner J. H., Weintraub D. A., 1998, AJ, 115, 1592
Kennicutt Jr. R. C., Lee J. C., Funes J. G. J. S., Sakai S., Akiyama S., 2008, ApJS, 178, 247
Langer N., Maeder A., 1995, A&A, 295, 685
Leitherer C., Ekström S., Meynet G., Schaerer D., Agienko K. B., Levesque E. M., 2014, ApJS, 212, 14
Levesque E. M., Massey P., Olsen K. A. G., Plez B., Meynet G., Maeder A., 2006, ApJ, 645, 1102
Levesque E. M., Massey P., Olsen K. A. G., Plez B., 2007, ApJ, 667, 202
Levesque E. M., Massey P., Plez B., Olsen K. A. G., 2009, AJ, 137, 4744
Massey P., 2002, ApJS, 141, 81
Massey P., Olsen K. A. G., 2003, AJ, 126, 2867
Massey P., Silva D. R., Levesque E. M., Plez B., Olsen K. A. G., Clayton G. C., Meynet G., Maeder A., 2009, ApJ, 703, 420
Mehner A. et al., 2017, A&A, 608, A124
Mehner A., Baade D., Rivinius T., Lennon D. J., Martayan C., Stahl O., Štefl S., 2013, A&A, 555, A116
Meixner M. et al., 2006, AJ, 132, 2268
Moe M., Di Stefano R., 2017, ApJS, 230, 15
Mokiem M. R. et al., 2007, A&A, 473, 603
Neugent K. F., Massey P., Skiff B., Drout M. R., Meynet G., Olsen K. A. G., 2010, ApJ, 719, 1784
Neugent K. F., Massey P., Skiff B., Meynet G., 2012, ApJ, 749, 177
Neugent K. F., Massey P., Hillier D. J., Morrell N., 2017, ApJ, 841, 20
Ohnaka K., Driebe T., Hofmann K.-H., Weigelt G., Wittkowski M., 2008, A&A, 484, 371
Pietrzyński G. et al., 2013, Nature, 495, 76
Pojmański G., 2002, AcA, 52, 397
Ramírez-Agudelo O. H. et al., 2013, A&A, 560, A29
Roche P. F., Aitken D. K., Smith C. H., 1993, MNRAS, 262, 301
Salpeter E. E., 1955, ApJ, 121, 161
Sandage A., Tammann G. A., 1974, ApJ, 191, 603
Shenar T. et al., 2016, A&A, 591, A22
Skrutskie M. F. et al., 2006, AJ, 131, 1163
Smith N., Owocki S. P., 2006, ApJ, 645, L45
Soszyński I. et al., 2009, AcA, 59, 239
Stothers R., 1969, ApJ, 155, 935
Stothers R., Chin C.-W., 1979, ApJ, 233, 267
Tabernero H. M., Dorda R., Negueruela I., González-Fernández C., 2018, MNRAS, 476, 3106
van Loon J. T., 2017, Mem. Soc. Astron. Ital., 88, 354

Downloaded from https://academic.oup.com/mnras/article-abstract/478/3/3138/4999916 by Liverpool John Moores University user on 24 September 2018

van Loon J. T., Groenewegen M. A. T., de Koter A., Trams N. R., Waters L. B. F. M., Zijlstra A. A., Whitelock P. A., Loup C., 1999, A&A, 351, 559
van Loon J. T., Cioni M.-R. L., Zijlstra A. A., Loup C., 2005a, A&A, 438, 273
van Loon J. T., Marshall J. R., Zijlstra A. A., 2005b, A&A, 442, 597
Wright E. L. et al., 2010, AJ, 140, 1868
Zaritsky D., Harris J., Thompson I. B., Grebel E. K., Massey P., 2002, AJ, 123, 855
Zaritsky D., Harris J., Thompson I. B., Grebel E. K., 2004, AJ, 128, 1606

APPENDIX A: BOLOMETRIC CORRECTIONS OF COOL SUPERGIANTS IN THE MAGELLANIC CLOUDS

Since we now have bolometric luminosities for each star in our sample, we can derive empirical bolometric corrections (BCs) as a function of spectral type. To do this, we take each star's photometry at Johnson *V*, DENIS-*I*, and 2MASS-K_S, dereddened according to the extinction law of Gordon et al. (2003). We do *not* remove any circumstellar component to the total extinction. Therefore, the BCs we provide should be applied to photometry *without* attempting to compensate for circumstellar extinction, which is notoriously difficult to estimate given its degeneracy with foreground extinction and the $T_{\rm eff}$ of the star. Our BCs already account for an average amount of circumstellar extinction for stars of the same spectral type and metallicity of the LMC and SMC.

At each spectral subtype, we take the average BC to be the median of all stars within ±0.5 subtypes. We have not estimated the BC at any subtype where we had less than five stars. We define the error at each subtype to be the standard deviation of stars in that bin within 2.5σ of the mean. This reduces the impact of the small number of outliers, typically caused by poor photometry. However, we note that there are some statistical outliers beyond these limits, particularly at later types.

Table A1. Average bolometric corrections as a function of spectral type for the two MCs. The filter systems are Johnson *V*, DENIS-*I*, and 2MASS K_s.

SpT	$BC_{\rm V}$	$BC_{\rm I}$	$BC_{\rm K}$
LMC			
K0-K3	-1.15 ± 0.23	0.50 ± 0.07	2.69 ± 0.11
K4	-1.16 ± 0.17	0.51 ± 0.07	2.69 ± 0.11
K5-K6	-1.19 ± 0.25	0.51 ± 0.06	2.70 ± 0.11
K7-M0	-1.43 ± 0.22	0.46 ± 0.10	2.77 ± 0.10
M1	-1.56 ± 0.21	0.42 ± 0.10	2.81 ± 0.07
M2	-1.72 ± 0.29	0.37 ± 0.14	2.85 ± 0.07
M3	-1.91 ± 0.39	0.31 ± 0.19	2.89 ± 0.10
M4	-2.12 ± 0.59	0.24 ± 0.20	2.94 ± 0.10
M5	-2.36 ± 0.63	0.16 ± 0.17	3.00 ± 0.09
SMC			
G5	-0.51 ± 0.27	0.75 ± 0.04	2.37 ± 0.24
G6	-0.57 ± 0.26	0.73 ± 0.08	2.40 ± 0.11
G7	-0.62 ± 0.20	0.71 ± 0.07	2.43 ± 0.09
G8	-0.68 ± 0.10	0.69 ± 0.05	2.46 ± 0.06
G9	-0.75 ± 0.10	0.67 ± 0.03	2.49 ± 0.05
K0	-0.81 ± 0.16	0.65 ± 0.05	2.52 ± 0.08
K1	-0.88 ± 0.11	0.63 ± 0.06	2.55 ± 0.05
K2	-0.95 ± 0.13	0.62 ± 0.07	2.58 ± 0.08
K3	-1.02 ± 0.25	0.60 ± 0.08	2.61 ± 0.12
K4	-1.10 ± 0.12	0.59 ± 0.12	2.64 ± 0.08
K5-K6	-1.18 ± 0.30	0.57 ± 0.12	2.67 ± 0.11
K7-M0	-1.43 ± 0.52	0.53 ± 0.11	2.76 ± 0.14
M1	-1.51 ± 0.30	0.52 ± 0.12	2.79 ± 0.05
M2	-1.60 ± 0.34	0.51 ± 0.24	2.82 ± 0.18
M3	-1.70 ± 0.46	0.50 ± 0.19	2.85 ± 0.07
M4	-1.79 ± 0.63	0.49 ± 0.15	2.88 ± 0.14

In Fig. A1 we compare our BCs at *V* and *K* to those of Elias et al. (1985) and L06. The BCs in Elias et al. were empirically derived, whereas those in L06 were determined from atmospheric models. While at face value there appears to be good agreement at *V* between all three studies and at *K* between this work and L06, one must keep in mind that the BCs of Elias et al. and Levesque et al. were defined for *unreddened* photometry. Therefore, removing a circumstellar component to the extinction of, e.g. $A_V \simeq 0.5$ prior to applying the BC would result in overestimating the luminosity from the *V*-band photometry by ∼0.2 dex.

Downloaded from https://academic.oup.com/mnras/article-abstract/478/3/3138/4999916 by Liverpool John Moores University user on 24 September 2018

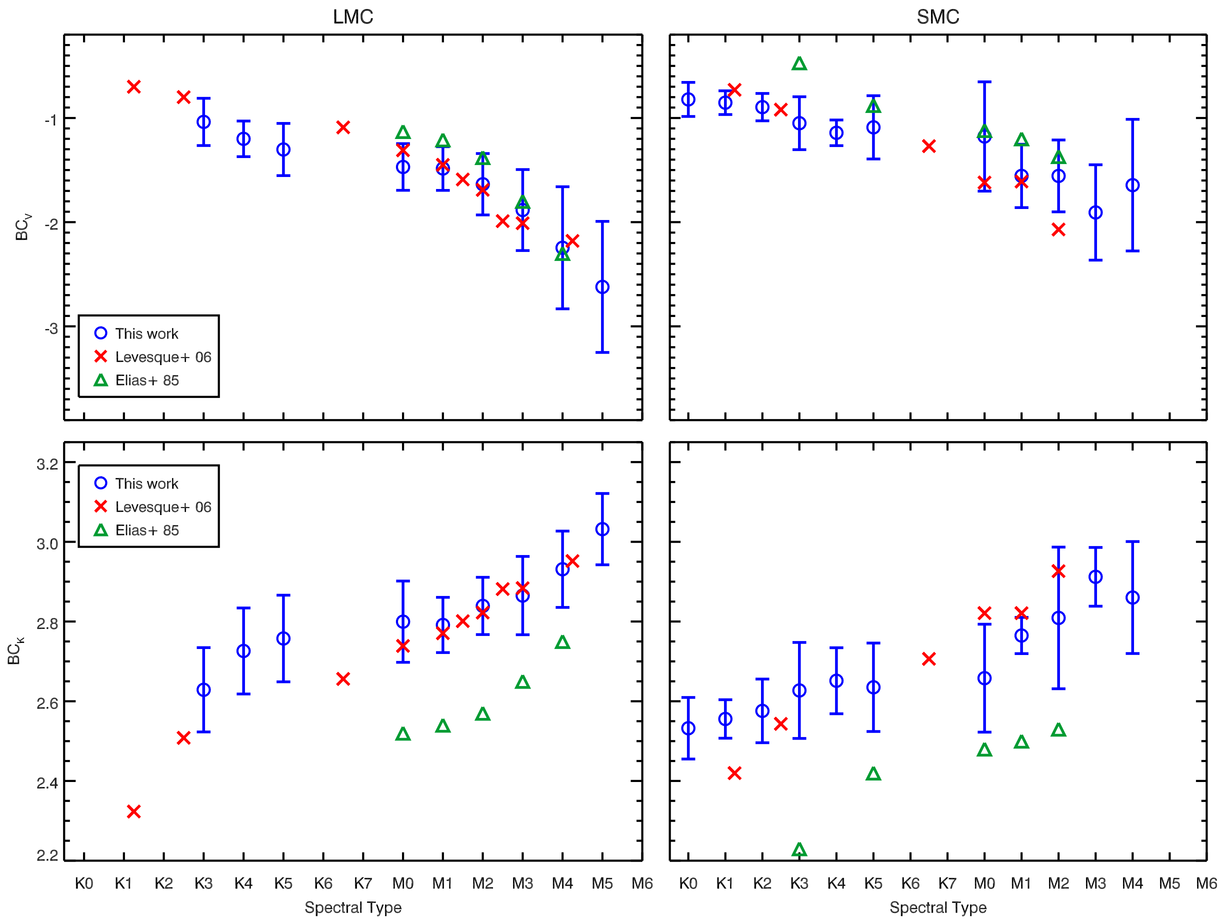

Figure A1. Bolometric corrections as a function of spectral type in the two MCs, compared to those measured by Elias et al. (1985) and Levesque et al. (2006).

This paper has been typeset from a TEX/LATEX file prepared by the author.

Downloaded from https://academic.oup.com/mnras/article-abstract/478/3/3138/4999916 by Liverpool John Moores University user on 24 September 2018